nature portfolio

https://doi.org/10.1038/s41558-022-01287-8

Supplementary information

Pronounced loss of Amazon rainforest resilience since the early 2000s

In the format provided by the authors and unedited

Supplementary Information for ‘Pronounced loss of Amazon rainforest resilience since the early 2000s’ by Chris A. Boulton, Timothy M. Lenton & Niklas Boers

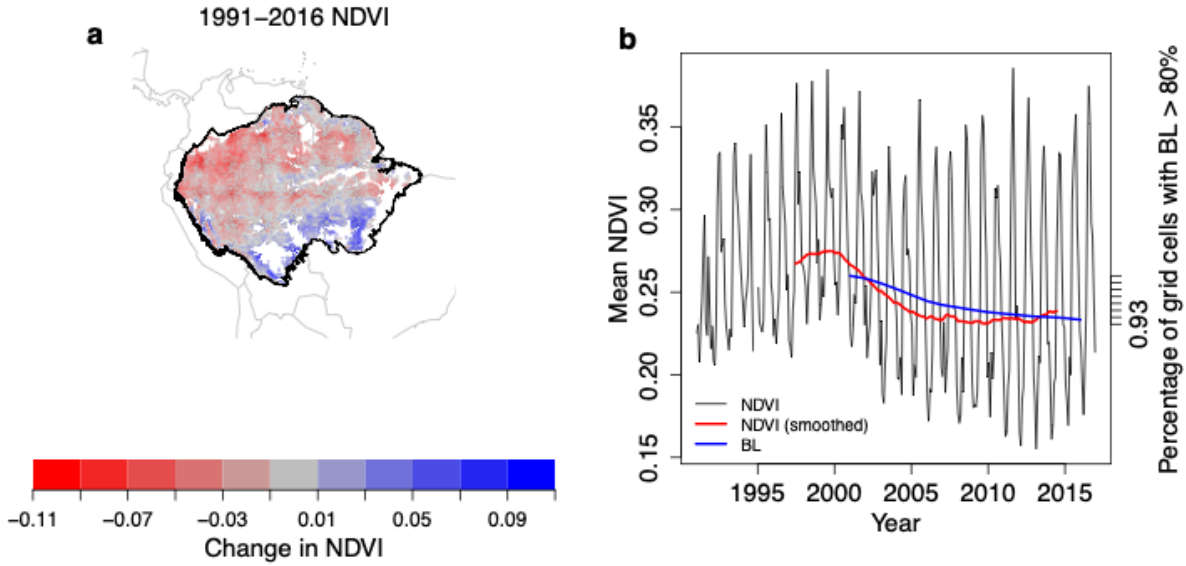

Supplementary Figure S1: Relationship between changes in NDVI and BL fraction in the Amazon Basin. (a) Change in AVHRR NDVI from 1991 to 2016 (difference between the 2012-2016 and 1991-1995 means) in forested (BL >= 80%) grid cells. (b) Time series of the median NDVI from these grid cells. Also shown in blue is the annual proportion of grid cells that have BL >= 80% given that they had BL >= 80% in 2001. Note that NDVI shows increases in the south-eastern parts of the Amazon basin, where both the BL fraction and VOD show decreases (see Figure 1 in the main text). Country outlines provided by the ‘maps’ package in R and Amazon Basin outline created from http://worldmap.harvard.edu/data/geonode:amapoly_ivb (see Methods).

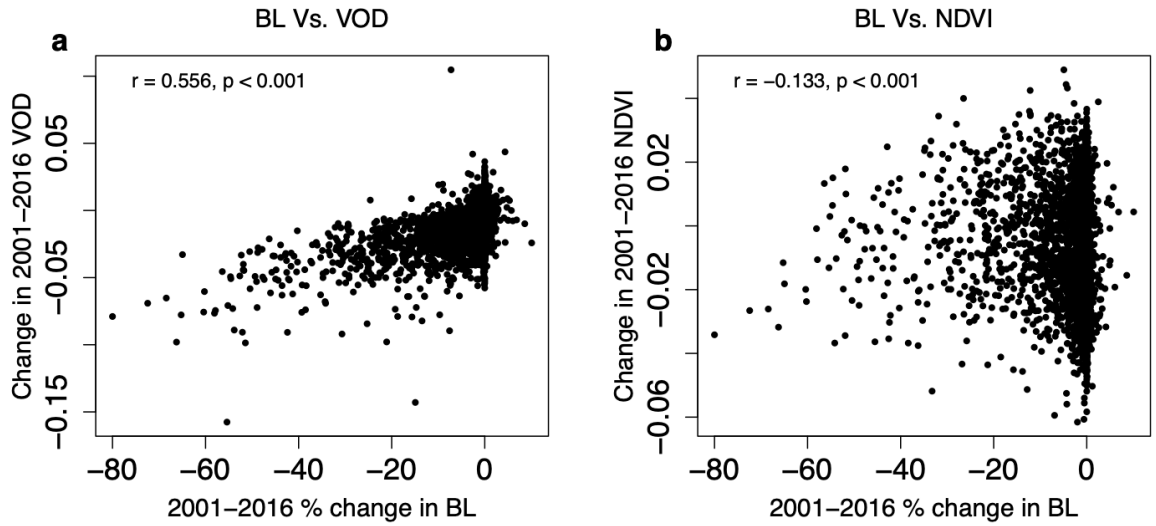

Supplementary Figure S2: Scatter plots of changes in vegetation variables in the Amazon basin. The 2001-2016 percent change in BL fraction for grid cells that have >= 80% BL in 2001 compared to the 2001-2016 change in (a) VOD and (b) NDVI. The correlations between the variables (r=0.556 and -0.133 respectively) show that VOD is a better measure of the BL fraction, and hence of actual forest cover rather than greenness, than NDVI.

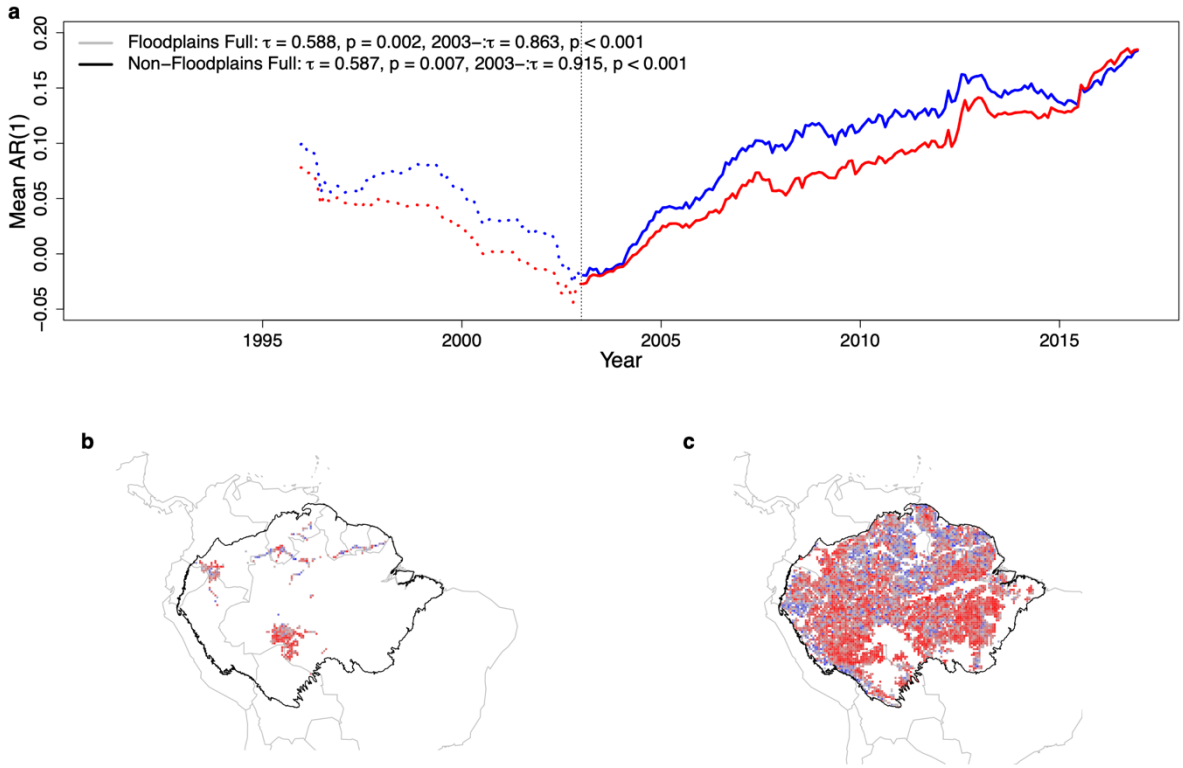

Supplementary Figure S3: Partitioning the grid cells by those that lie within Amazon basin floodplains. Floodplains were determined from part of the NASA Large Scale Biosphere-Atmosphere Experiment (see Methods). (a) The mean AR(1) time series from those grid cells within (blue) and outside (red) floodplains show no discernible differences, with only a slightly lower increase in floodplain AR(1) since 2003 (Kendall τ values for the full time series, floodplains: 0.588, non-floodplains: 0.587; correspondingly from 2003 onwards, floodplains: 0.863, non-floodplains: 0.915). (b) and (c) show the spatial pattern in floodplain and non-floodplain Kendall τ values, respectively. Country outlines provided by the 'maps' package in R and Amazon Basin outline created from http://worldmap.harvard.edu/data/geonode:amapoly_ivb (see Methods).

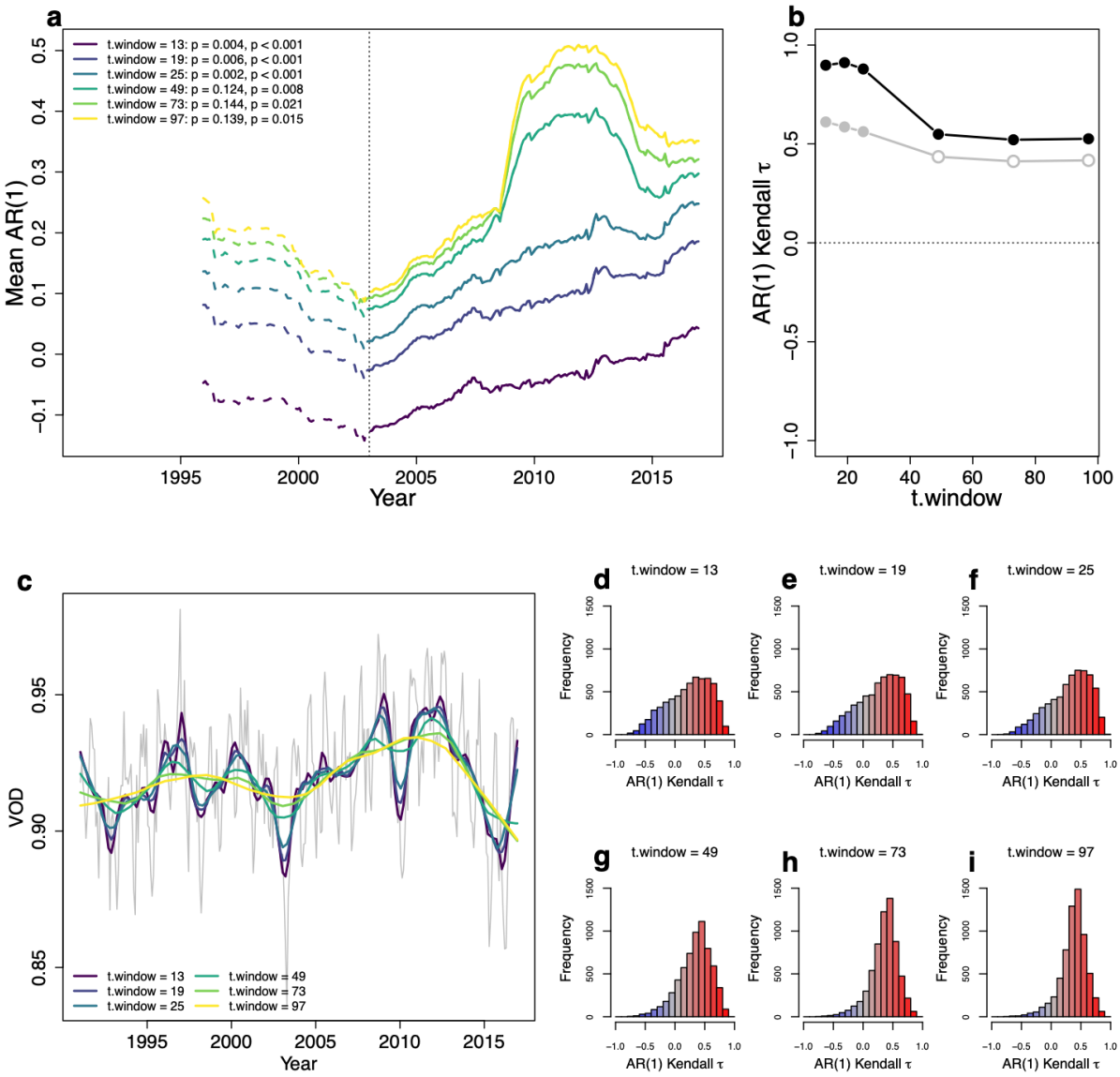

Supplementary Figure S4: Tests of robustness for detrending the VOD time series. In the main paper, VOD time series are detrended and de-seasonalised using the stl() function in R (see Methods). Here we vary the time window (t.window) used to calculate the long term trend, whilst keeping the seasonal window periodic. In the main paper, t.window=19 months. (a) The mean AR(1) time series for each choice of t.window is shown. This is comparable to Fig. 2a in the main paper. (b) The Kendall τ values of the mean AR(1) time series from the full time series (grey), and from 2003 onwards (black) for each t.window are all positive. Closed circles denote that Kendall τ values are significantly positive ($p < 0.05$). (c) The trends removed based on t.window for a typical grid cell VOD time series (shown behind in grey). (d-i) The histogram of point-level Kendall τ values from 2003 onwards for the choices of t.window showing that the skew towards positive tendencies in AR(1) found in the main paper (when t.window = 19) is robust and becomes even more pronounced for longer windows.

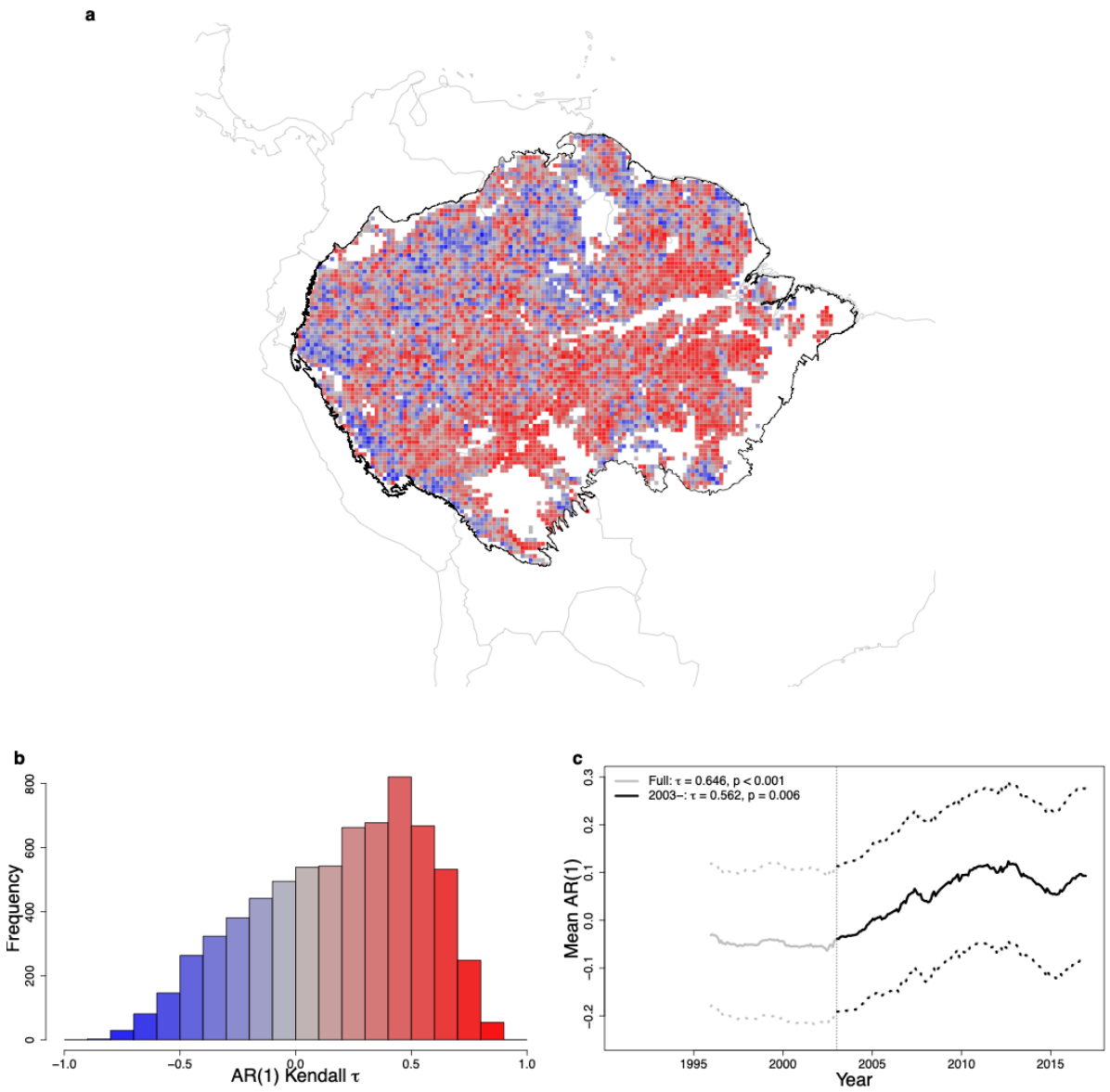

Supplementary Figure S5: Recreation of Figure 2 using s.window=13 rather than 'periodic' in the stl() function used to detrend individual time series. (a) A map of the Kendall τ values of individual grid cells from 2003. (b) Histogram of the Kendall τ values for the Amazon basin, considering data from 2003 onwards. (c) Mean VOD AR(1) time series (solid line) along with +/- 1 standard deviation (dotted lines) created from grid cells that have BL fraction above 80% in the Amazon basin and also contain no human land use (see main text and Methods). The full AR(1) time series from 1991 (grey) has a Kendall τ value of 0.646 ($p < 0.001$) and from 2003 (black), a value of 0.562 ($p = 0.006$). Note that the AR(1) values are plotted at the end of each 5-year sliding window. Country outlines provided by the 'maps' package in R and Amazon Basin outline created from http://worldmap.harvard.edu/data/geonode:amapoly_ivb (see Methods).

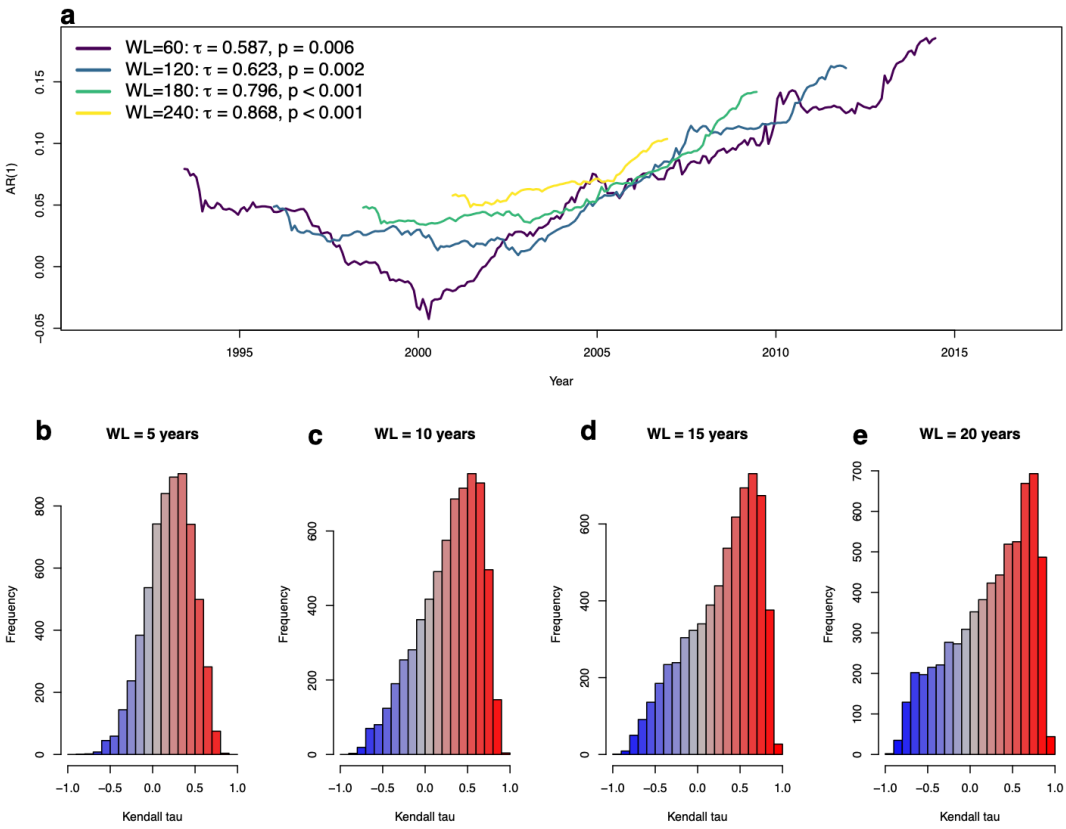

Supplementary Figure S6: Robustness of VOD AR(1) to choice of window length. (a) the mean Amazon Basin VOD AR(1) time series for a selection of window lengths, 5 years (as in Figure 2), 10 years, 15 years, and 20 years. For a clearer comparison of window lengths, we plot the AR(1) values in the middle of the window used to calculate them. Histograms (b)-(f) show the individual grid cell Kendall tau values for these choices of window lengths, showing a robust increase in AR(1) across the region, regardless of window length.

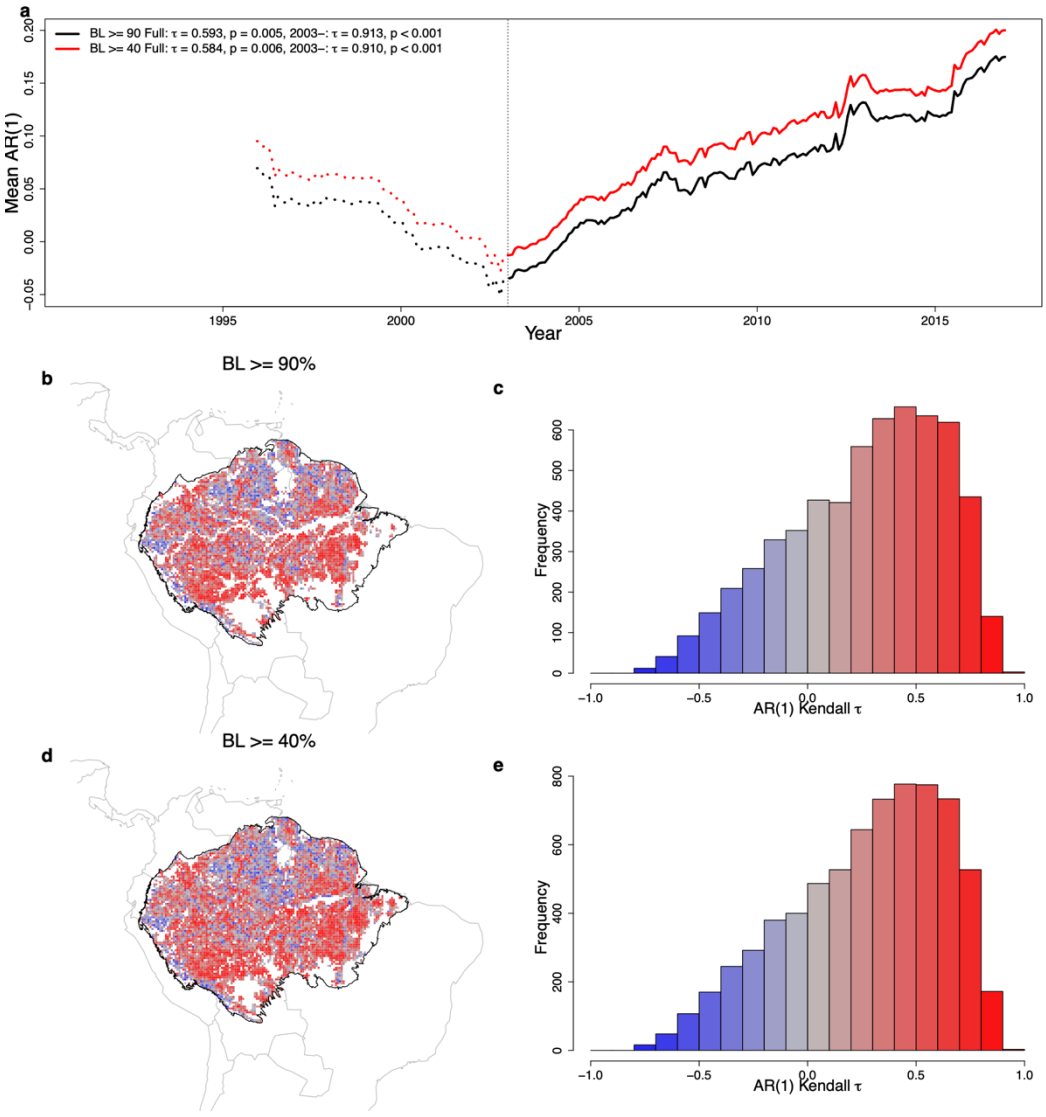

Supplementary Figure S7: Mean overall AR(1) signals for the Amazon Basin when varying the threshold of BL fraction that determines forest. (a)-(c) recreation of Figure 2 but only using grid cells with BL >= 90%. Also shown in (a) is the AR(1) time series for grid cells where BL >= 40%. (d) and (e) the same as (b) and (c) but with grid cells with BL >= 40%. Country outlines provided by the 'maps' package in R and Amazon Basin outline created from http://worldmap.harvard.edu/data/geonode:amapoly_ivb (see Methods).

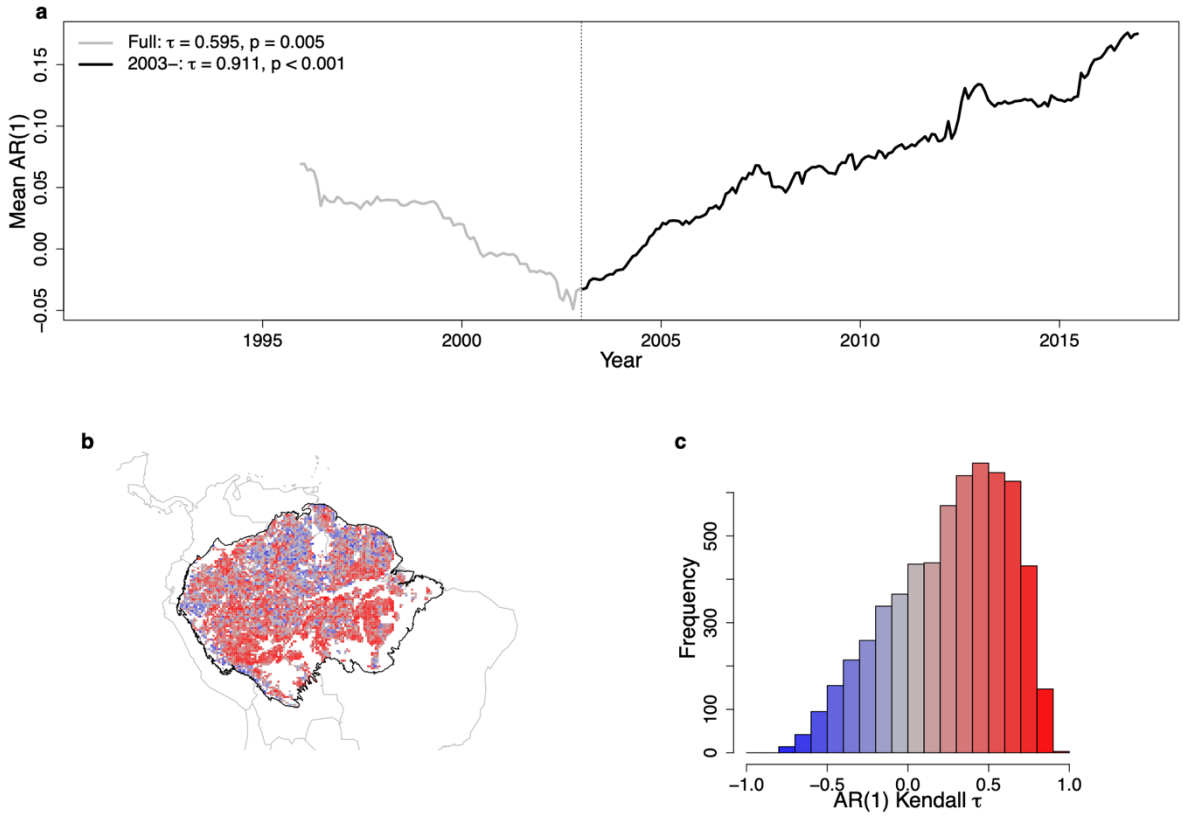

Supplementary Figure S8: VOD AR(1) signals observed in grid cells that exhibit BL >= 80% from 2001-2016. (a) mean AR(1) time series is shown for those grid cells that are classed as forest for the full period we have data on BL fraction and no human land use (see main text and Methods). (b) and (c) show the individual grid cell Kendall tau values from 2003 onwards, for comparison with Figure 2. This confirms that the loss of resilience we infer cannot be explained solely based on the reduction of BL fraction. Country outlines provided by the 'maps' package in R and Amazon Basin outline created from http://worldmap.harvard.edu/data/geonode:amapoly_ivb (see Methods).

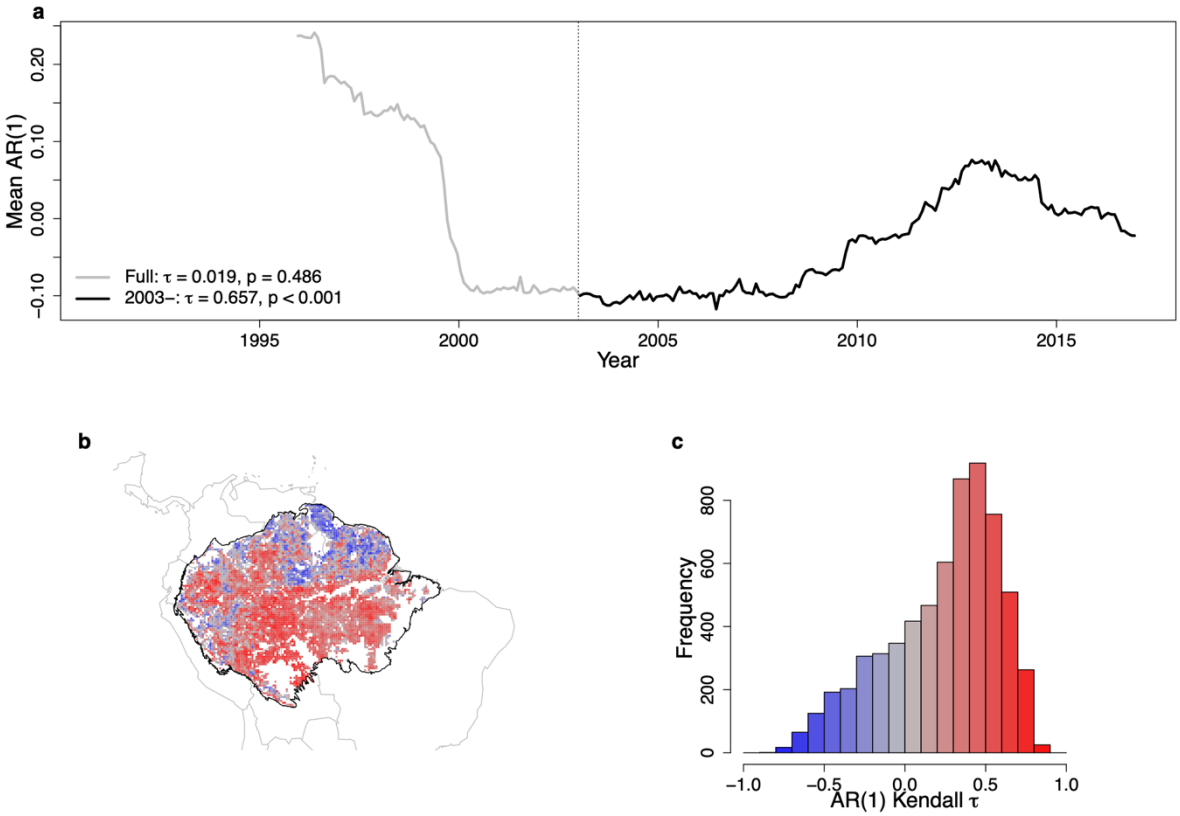

Supplementary Figure S9: Changes in Amazon vegetation resilience as measured by NDVI since the 1991 and from the early 2000s. (a) Mean NDVI AR(1) time series created from grid cells that have BL fraction above 80% in the Amazon basin. The full AR(1) time series from 1991 (grey) has a Kendall τ value of 0.008 ($p = 0.491$) and from 2003 (black), a value of 0.647 ($p < 0.001$). The tendency of the full time series is strongly influenced by the strong decrease at the start. (b) A map of the Kendall τ values of individual grid cells from 2003, shown with contours of MAP (mm/year) over the same time period. (c) A histogram of the pointwise Kendall τ values from the map. Country outlines provided by the 'maps' package in R and Amazon Basin outline created from http://worldmap.harvard.edu/data/geonode:amapoly_ivb (see Methods).

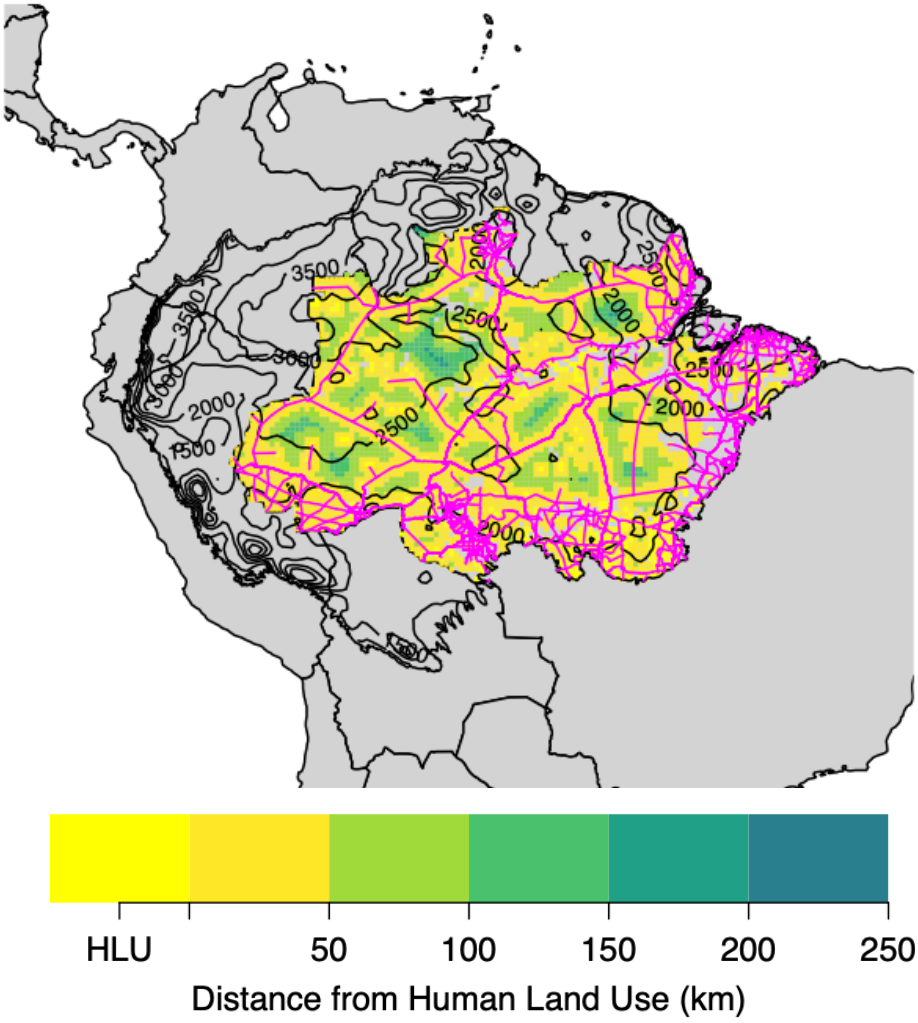

Supplementary Figure S10: Brazilian Amazon distances from human land use or roads. The distances from human land use or Brazilian federal or state roads (see Methods) are shown for the subset of Amazonian grid cells where 2001 BL fraction >= 80% and there is no human land use (see main text and Methods). The colour scale matches the one in Figure 3c such that the same distances are the same colour. As in all panels of Figure 3, human land use grid cells are shown in yellow, roads in magenta, and contours show MAP from 1991-2016. Country outlines provided by the 'maps' package in R and Amazon Basin outline created from http://worldmap.harvard.edu/data/geonode:amapoly_ivb (see Methods).

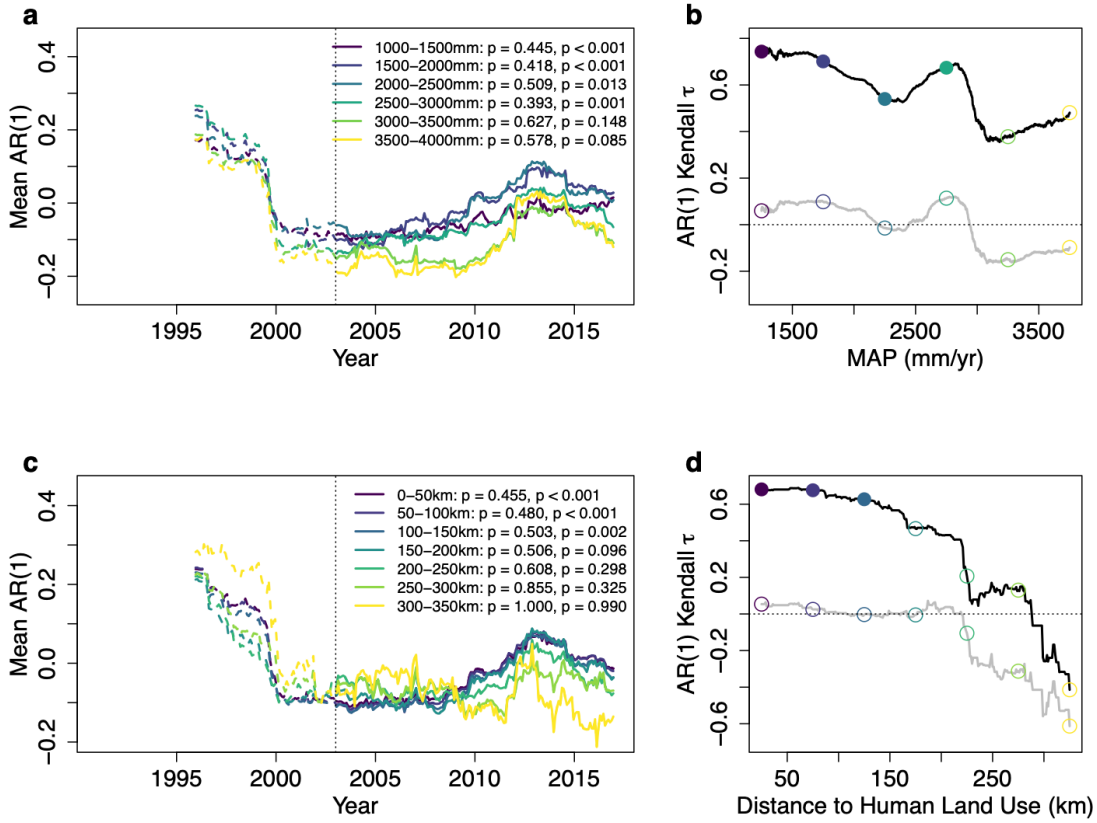

Supplementary Figure S11: The relationship between annual rainfall sums and distance from human land use, and vegetation resilience as measured by NDVI. (a) NDVI AR(1) time series for 6 500mm MAP-bands from 1991 (dashed lines) and from 2003 (solid lines). The legend in the panel shows the p-values for tendencies of the full time series, and from 2003 onwards respectively (when measured by Kendall τ). (b) Full NDVI AR(1) Kendall τ series for a sliding MAP-band, from 1991 (grey) and from 2003 (black). Red circles show the results from panel (a) and are closed if the Kendall τ value is significantly positive ($p < 0.05$) and open otherwise. The tendency of these series (also measured by the Kendall τ rank correlation coefficient) are -0.457 and -0.599, respectively, confirming there is generally a more severe decrease in resilience with a decrease in rainfall. Although heavily influenced by the large decline in AR(1) at the beginning of the time series, over the whole time period, the Kendall τ series suggests that there is an increase in resilience at higher MAP values as the AR(1) is decreasing overall ($\tau < 0$). (c) and (d) show the same as (a) and (b) but using the distance from human land use rather the MAP on a sliding window. The tendency of the series in (d) are -0.680 for the full time series, and -0.896 from 2003 onwards, showing there is a more severe decrease in resilience with increasing proximity to human land use.

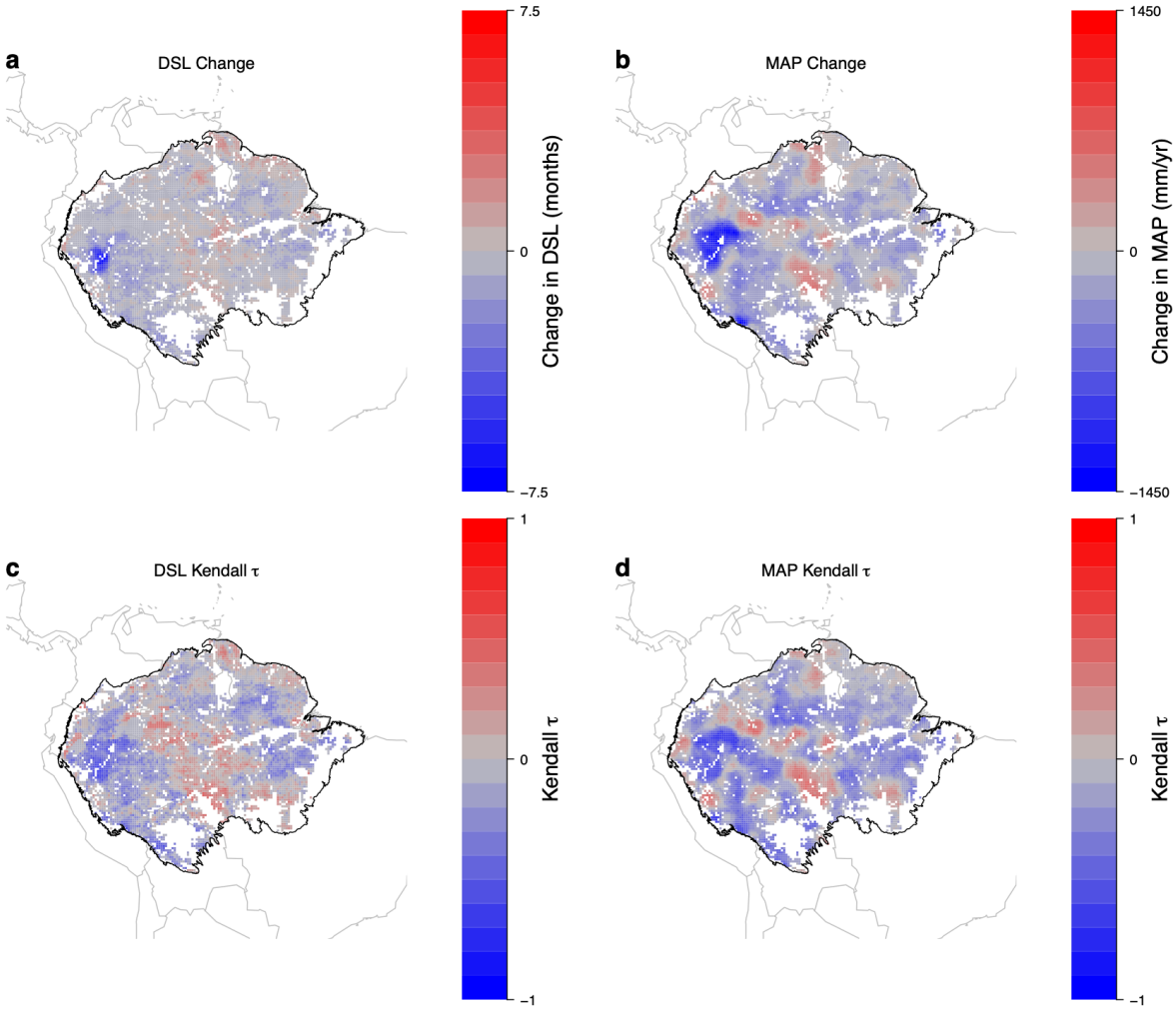

Supplementary Figure S12: The change in DSL and MAP from 2003. (a). The change in DSL (the number of months in a year with precipitation below 100mm) over the time period used to calculate AR(1) time series from 2003 (due to the 60-month sliding window, this is the difference in mean DSL from Jan 1998 - Dec 2002 and Jan 2012 – Dec 2016). (b) The change in MAP over the same period. (c) and (d) show the Kendall τ values from the time series of these variables at each grid cells respectively. None of these measures are correlated with the VOD AR(1) Kendall τ values (Spearman's ρ=-0.08, 0.04, -0.02 and 0.02 respectively). Country outlines provided by the 'maps' package in R and Amazon Basin outline created from http://worldmap.harvard.edu/data/geonode:amapoly_ivb (see Methods).

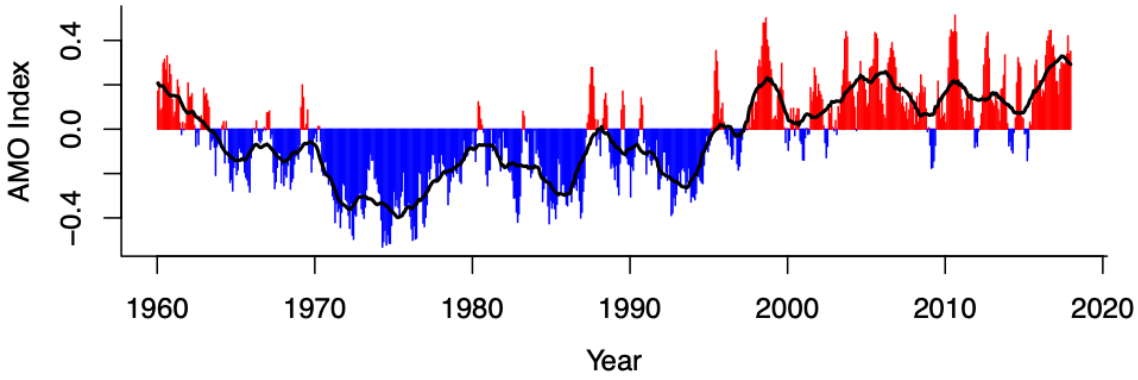

Supplementary Figure S13: Time series the Atlantic Multidecadal Oscillation (AMO) Index. Time series is coloured blue if negative and red if positive. A Kernal smoothing function with bandwidth equal to 2 is used to show longer term behaviour (solid black line). The Methods section provides information on data source.

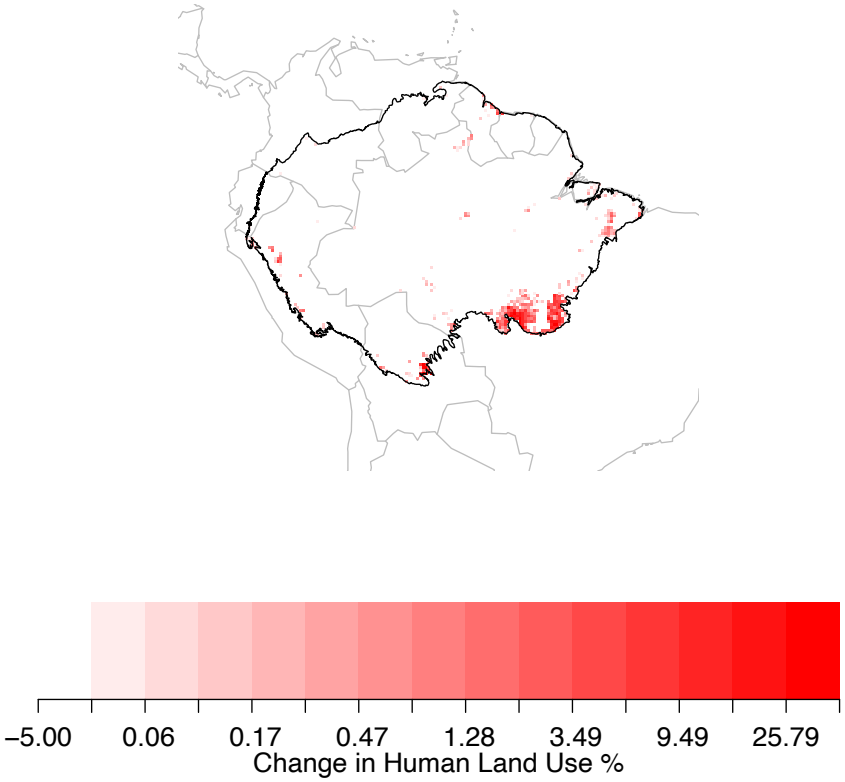

Supplementary Figure S14: The change in human land use over time. (a) The grid cell percentage change in human land use (as defined in the Methods using the MODIS Land Cover Product from 2001 to 2016 in the Amazon Basin. Country outlines provided by the 'maps' package in R and Amazon Basin outline created from http://worldmap.harvard.edu/data/geonode:amapoly_ivb (see Methods).

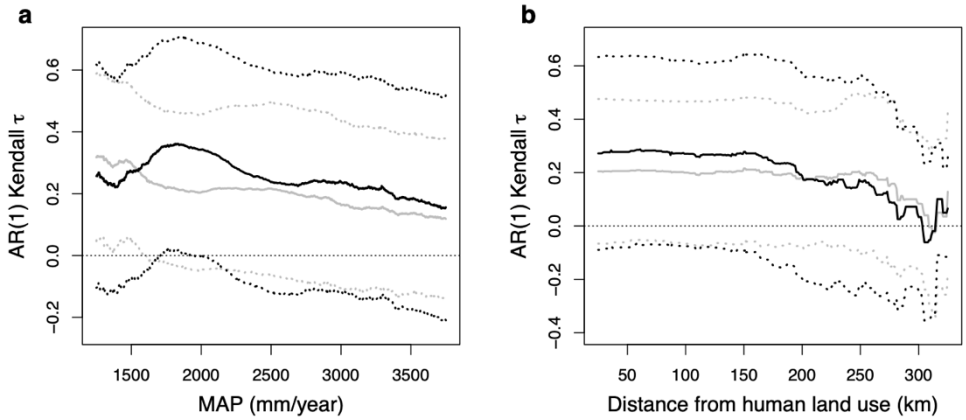

Supplementary Figure S15: Kendall τ series calculated from an alternative method. Series are created by taking the mean of the individual Kendall τ values, computed from the AR(1) time series at individual grid cells in the MAP- and distance-band, rather than creating a mean AR(1) time series for each band first (see Methods). Series are shown in grey for the whole time period, and black for 2003 onwards. Tendencies (also measured by Kendall τ) respectively are as follows: (a) VOD AR(1) Kendall τ Vs. MAP: τ=-0.856, -0.652, (b) VOD AR(1) Kendall τ Vs. human land use distance: τ=-0.639, -0.827. In both plots, a +/- 1 standard deviation from the mean is shown with dotted lines. This is possible using this alternative method as we are taking τ values from a distribution rather than computing them from a single time series as we do in the main paper.

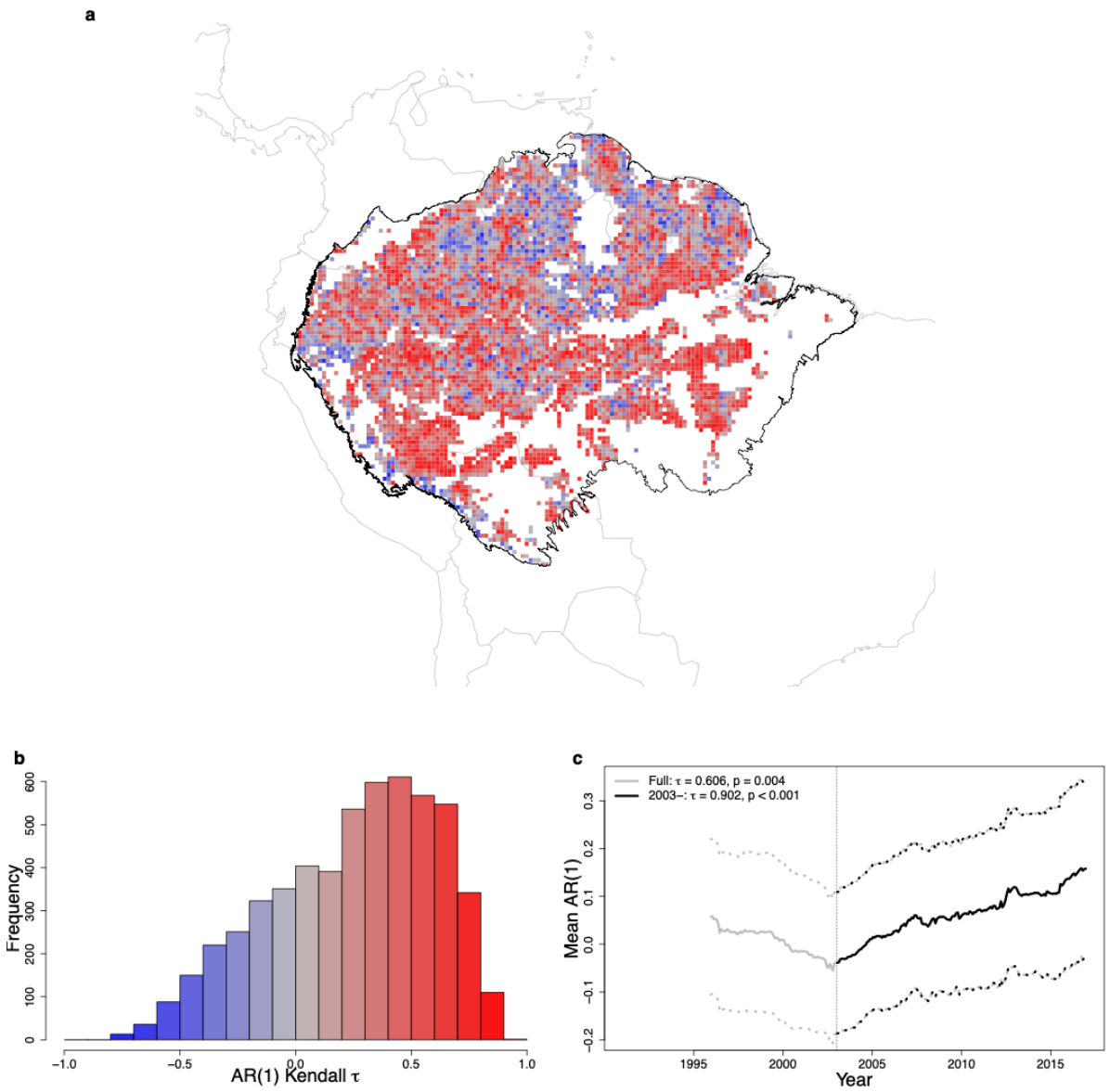

Supplementary Figure S16: Recreation of Figure 2 using the grid cells that have no exhibited forest loss since 2001 according to the Hansen forest loss dataset. (a) A map of the Kendall τ values of individual grid cells from 2003. (b) Histogram of the Kendall τ values for the Amazon basin, considering data from 2003 onwards. (c) Mean VOD AR(1) time series (solid line) along with +/- 1 standard deviation (dotted lines) created from grid cells that have exhibited no more than a 5% area of forest loss since 2001 (see Me. The full AR(1) time series from 1991 (grey) has a Kendall τ value of 0.606 (p = 0.004) and from 2003 (black), a value of 0.902 (p < 0.001). Note that the AR(1) values are plotted at the end of each 5-year sliding window. Country outlines provided by the 'maps' package in R and Amazon Basin outline created from http://worldmap.harvard.edu/data/geonode:amapoly_ivb (see Methods).

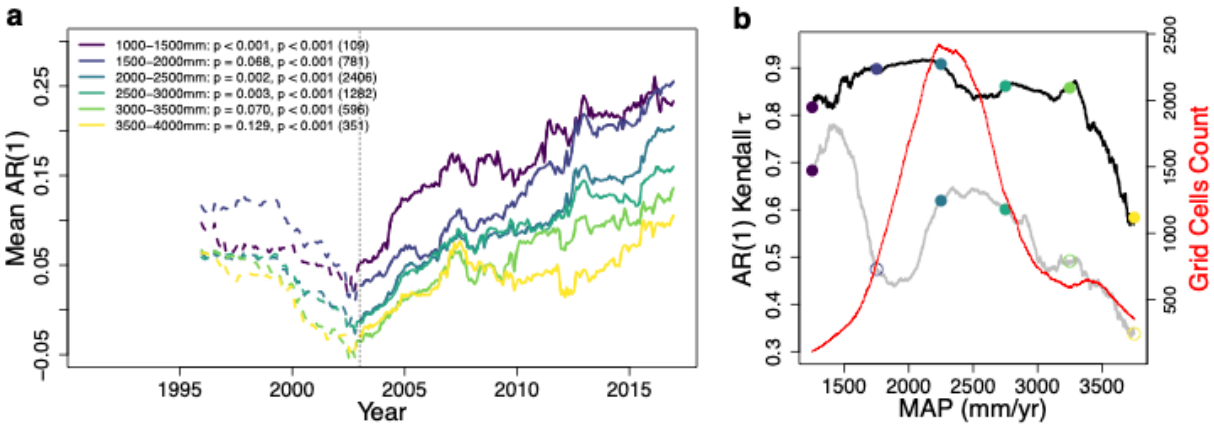

Supplementary Figure S17: Recreation of Figure 4 using the grid cells that have no exhibited forest loss greater than an area of 5% since 2001 according to the Hansen forest loss dataset. (a) VOD AR(1) time series for 500mm MAP-bands from 1996 (including data going back to 1991; dashed lines) and from 2003 (including data going back to 1998; solid lines). The p-values of the trend significance test (see Methods) are given in the legend; from 2003 onwards, they are all smaller than 0.001. (b) VOD AR(1) Kendall τ series for a sliding MAP-band with a width of 500mm, from 1996 (grey) and from 2003 (black). Circles are coloured according to the corresponding time series shown in (a) and closed if the Kendall τ value is significantly positive ($p < 0.05$) and open otherwise. The tendency of the relationships in (b) are $\tau = -0.485$ (grey) and $\tau = -0.389$ (black), confirming there is a more severe decrease in resilience with lower rainfall values. The number of grid cells used to calculate the AR(1) time series and thus the Kendall τ values are shown in red in (b). This never falls below 100 grid cells and so we can be confident in the mean estimation of the AR(1) time series. Note that the AR(1) values are plotted at the end of each 5-year sliding window.

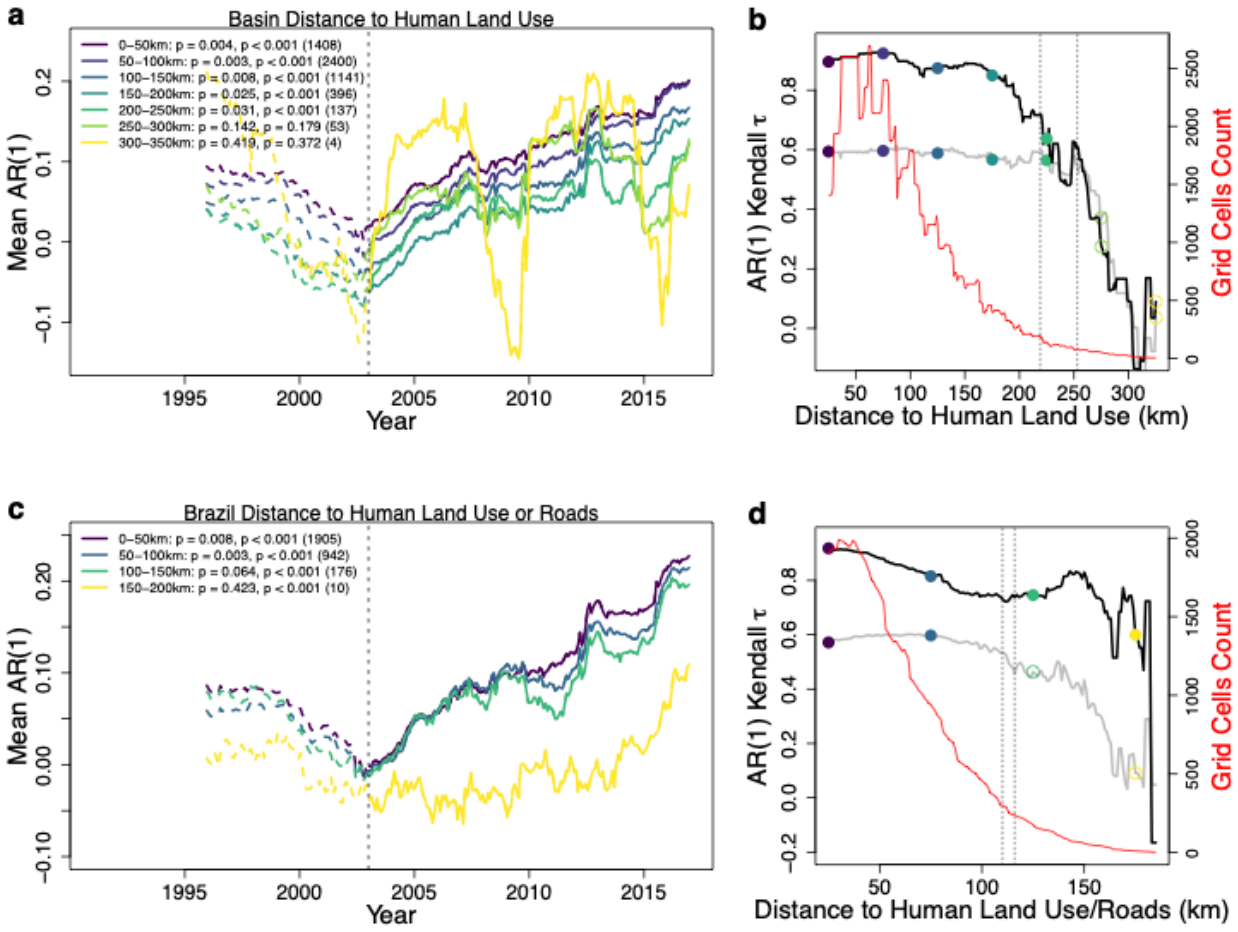

Supplementary Figure S18: Recreation of Figure 5 using the grid cells that have no exhibited forest loss greater than an area of 5% since 2001 according to the Hansen forest loss dataset. (a) VOD AR(1) time series for 50km bands measuring the minimum distance a forested grid cell is from a grid cell with human land use (defined in the Methods from the MODIS Land Cover product and shown in Fig. S6), from 1996 (dashed lines, these include data going back to 1991 due to the 5-year sliding windows used to estimate the AR(1)) and from 2003 (solid lines, including data going back to 1998), with the significance of these respective tendencies shown in the legend (see Methods). (b) VOD AR(1) Kendall τ series for the sliding 50km bands, from 1996 (grey, again including data going back to 1991) and from 2003 (black, including data going back to 1998). Circles are coloured according to the corresponding time series in (a) and are closed if the Kendall τ value is significantly positive ($p < 0.05$) and open otherwise. The tendency of these relationships are $\tau = -0.704$ (grey) and $\tau = -0.819$ (black), showing that there is a more severe decrease in resilience with increasing proximity to human land use. The number of grid cells used to calculate the AR(1) time series and thus the Kendall τ values are shown in red in (b), with vertical dotted lines denoting where there are 100 and 50 grid cells available for the calculation. The number of grid cells used in the calculation of the time series in (a) are shown in brackets in the legend. (c,d): The same as (a) and (b) but for the subset of grid cells in Brazil, where reliable road data is available (as shown in Fig. S9). For this case, where the distances from any given forested grid cell to human land use or roads are computed, the trends in the Kendall τ series are $\tau = -0.765$ and $\tau = -0.692$ respectively.

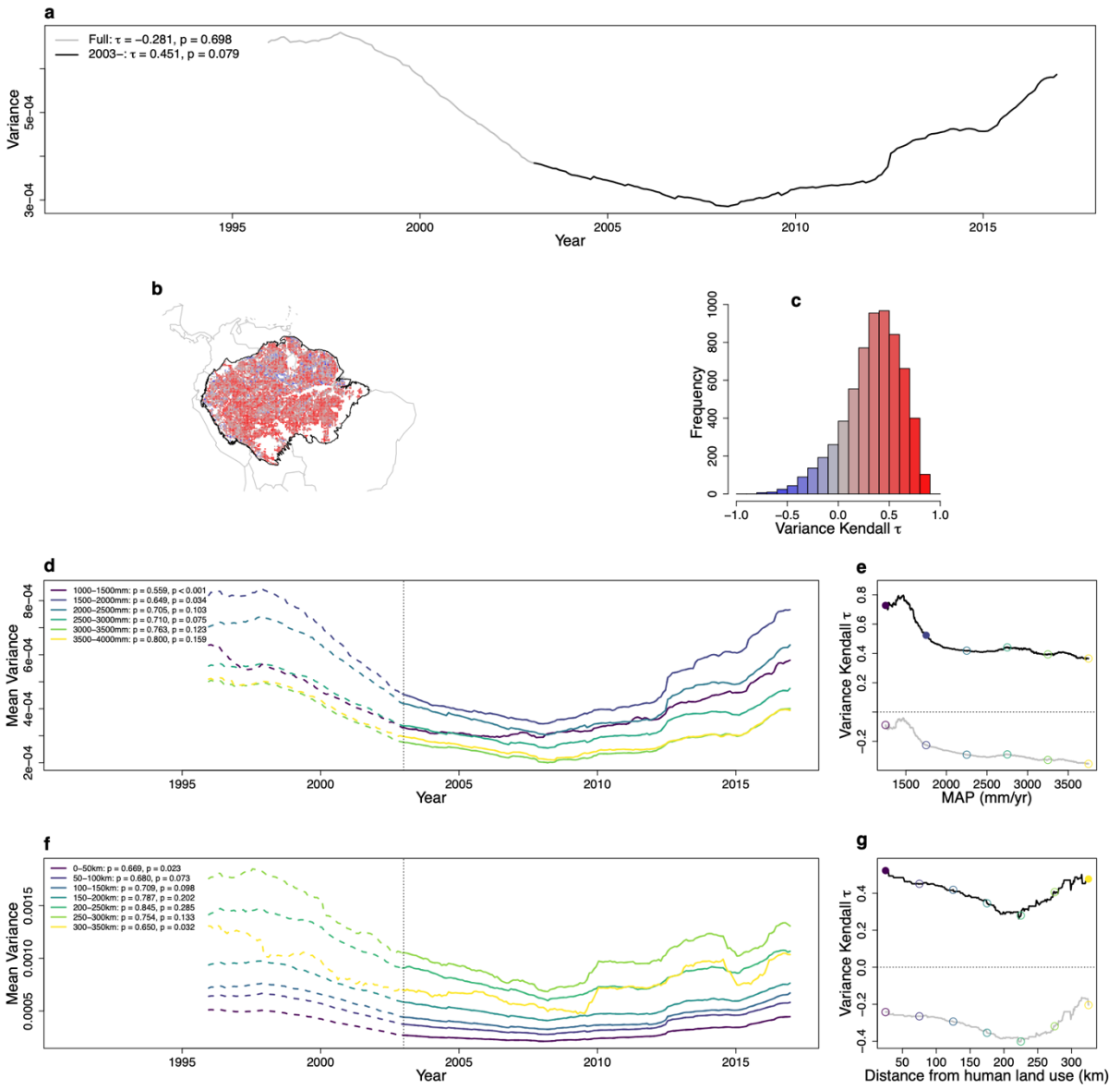

Supplementary Figure S19: Changes in Amazon resilience as measured from variance of VOD over time. (a) Time series of mean regional VOD variance show a non-significant increase in variance from 2003. (b,c) Grid cell Kendall tau values of VOD variance from 2003, where increases are generally seen across the region. (Compare (a)-(c) to Figure 2.) (d,e) Mean variance time series by MAP-bands, and corresponding Kendall τ values for all MAP-bands. Solid lines are shown from 2003 onwards, with p-values in the legend referring to the Kendall τ values for the full time series, and from 2003 onwards, respectively. The values are shown as red circles in (e) and are closed if $p < 0.05$ or open otherwise. There is a decrease in τ for higher MAP bands (in (e) for the full series $\tau = -0.864$ and from 2003 onwards $\tau = -0.737$). For the full time series, negative trends in variance suggest resilience is being gained, but this is influenced by the high variance at the start of the time series. (Compare (d) and (e) to Figure 3.) (f,g) Mean variance time series by bands of distance from human land use (in (g) $\tau = -0.293$ and -0.323 respectively). Country outlines provided by the 'maps' package in R and Amazon Basin outline created from http://worldmap.harvard.edu/data/geonode:amapoly_ivb (see Methods).

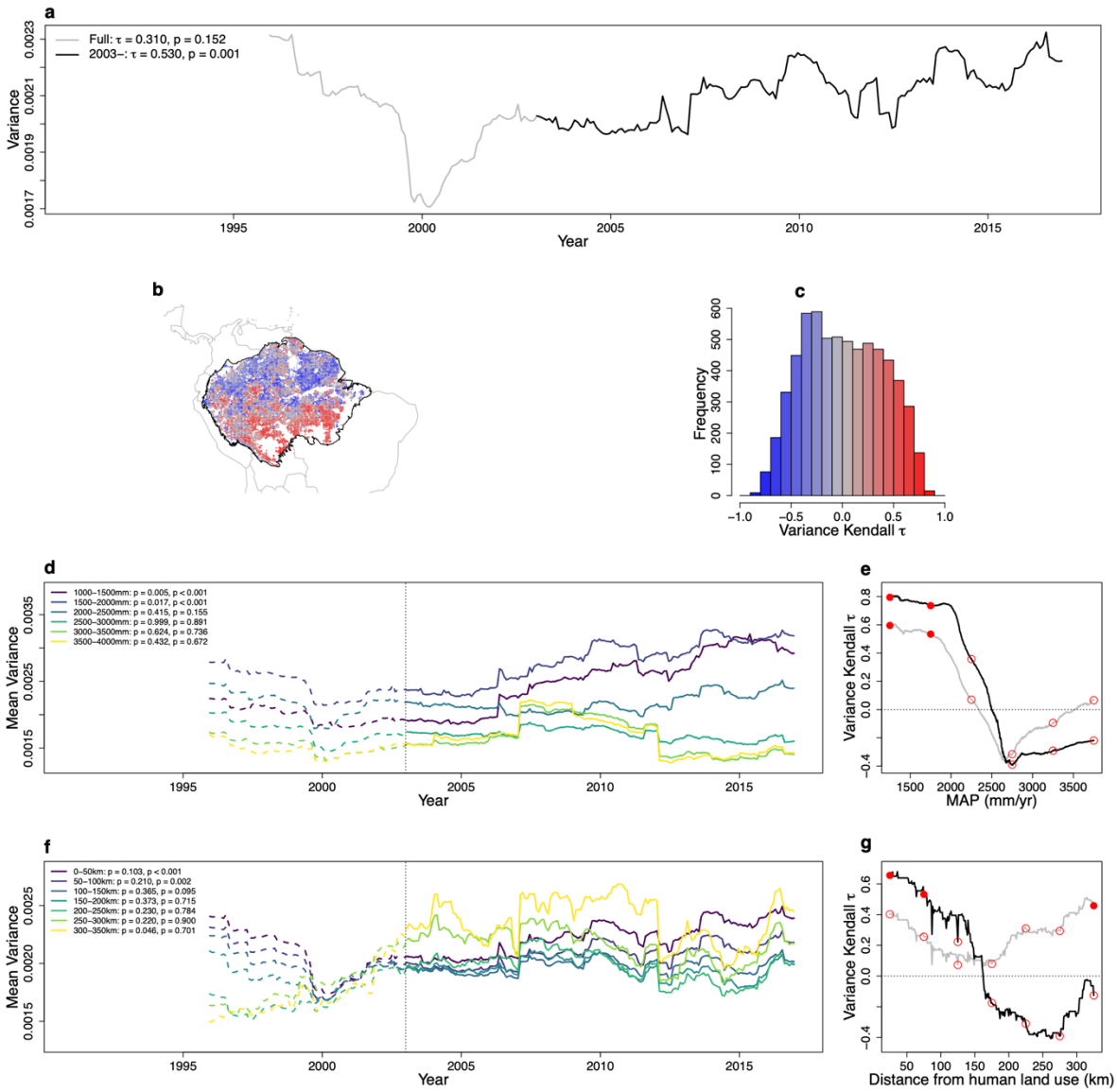

Supplementary Figure S20: Changes in Amazon resilience as measured from variance of NDVI over time. (a) Time series of mean regional NDVI variance showing a significant increase from 2003. (b,c) Grid cell Kendall τ values of VOD variance from 2003, where increases are generally in the south of the region, and decreases in the north. (d,e) Example mean variance time series by MAP-bands, and corresponding Kendall τ values for all MAP-bands. Solid lines are shown from 2003 onwards, with p-values in the legend referring to the Kendall τ values for the full time series, and from 2003 onwards respectively. The values are shown as red circles in (e) and are closed if $p < 0.05$ or open otherwise. There is a clear decrease in τ for higher MAP bands (full series τ = -0.452, from 2003 onwards τ = -0.594). Negative τ values, observed for MAP >2500mm, suggest resilience is being gained; compare panels (d,e) here to Figure 3 of the main paper. (f,g) Mean variance time series for bands of distance from human land use (in (g) τ = 0.240 and -0.701). Despite a decrease in the intensity of resilience loss with increasing distance for the full time series, resilience loss is observed across the full time series. Country outlines provided by the 'maps' package in R and Amazon Basin outline created from http://worldmap.harvard.edu/data/geonode:amapoly_ivb (see Methods).

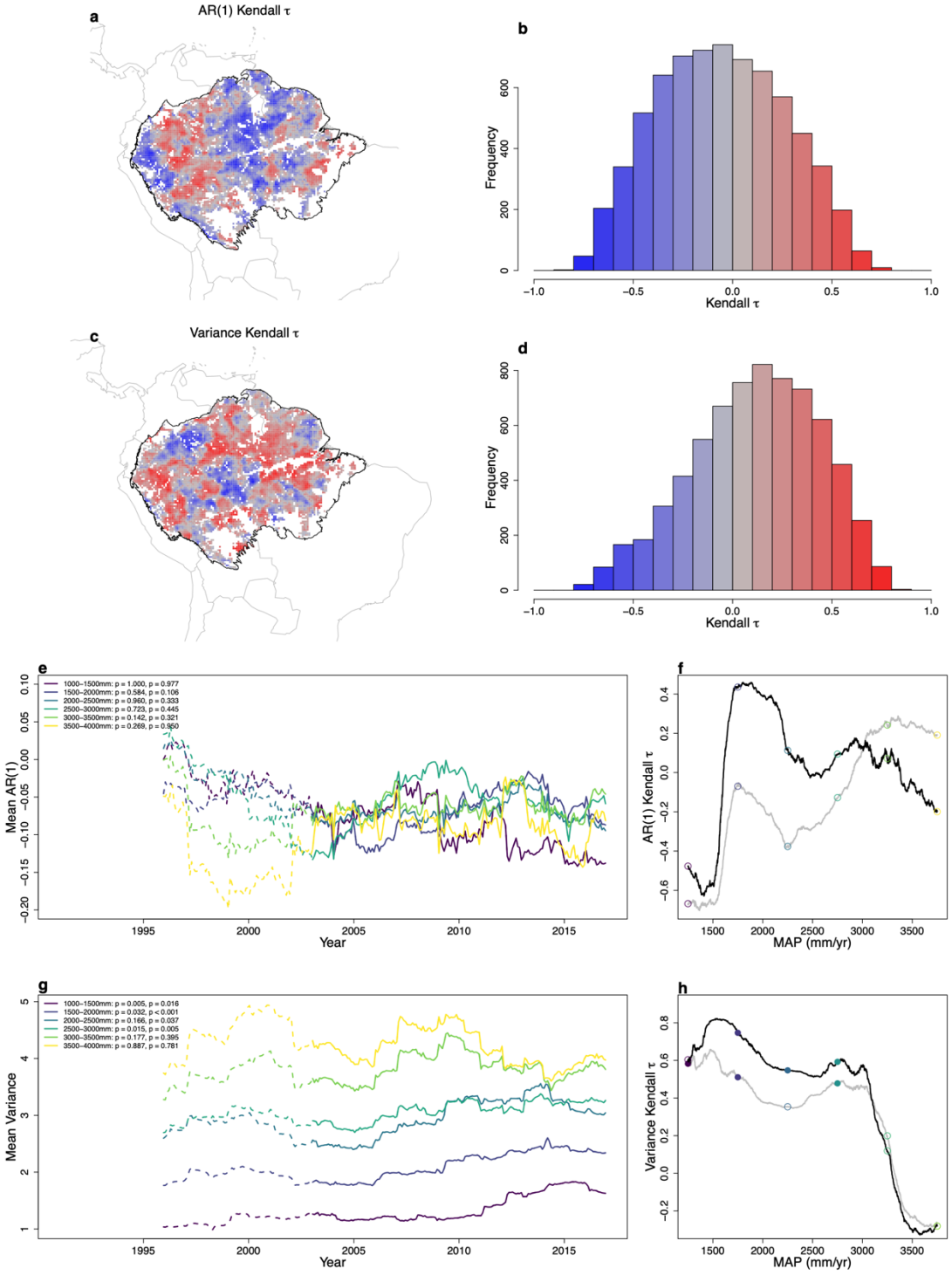

Supplementary Figure S21: Resilience indicators measured on precipitation time series. Precipitation time series are first detrended using STL-decomposition (as for the VOD and NDVI time series) and then AR(1) and variance are calculated on a moving window of 5 years. (a) and (b) show the Kendall tau values for AR(1) and (c) and (d) for variance. (e) and (f) show the time series for different MAP-bands and corresponding Kendall tau values (as in Figure 3 for VOD), and (g) and (h) shows the same for variance. These patterns do not match those observed in the VOD or NDVI time series. Country outlines provided by the 'maps' package in R and Amazon Basin outline created from http://worldmap.harvard.edu/data/geonode:amapoly_ivb (see Methods).

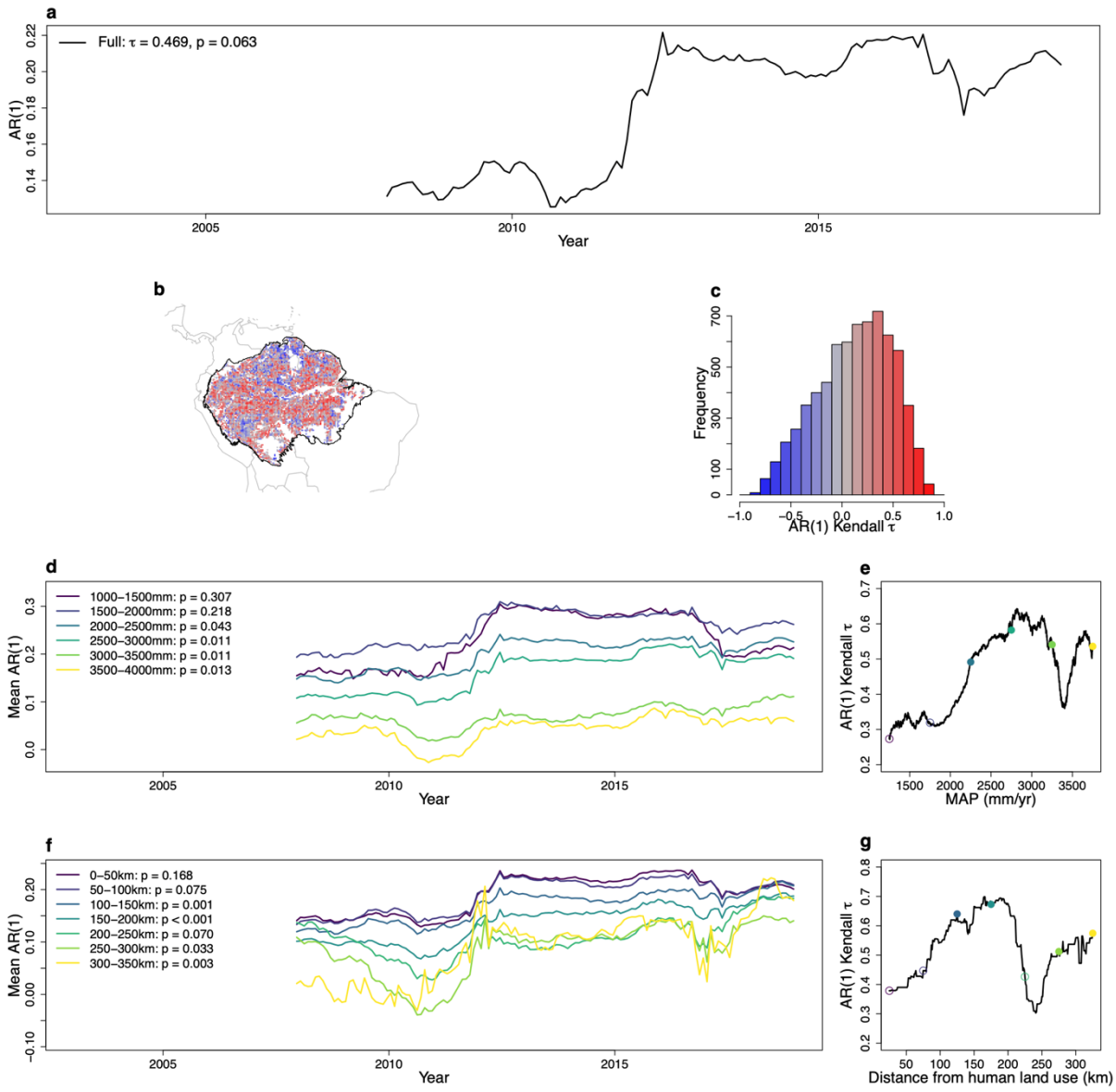

Supplementary Figure S22: Resilience signals calculated on the C-Band product of the VODCA. (a)-(c) Amazon Basin (BL >= 80%) mean AR(1) signals and associated Kendall τ values (as in Figure 2 for the Ku-Band product). (d) and (e) C-Band AR(1) signals and associated Kendall tau values calculated per MAP-band (as in Figure 3 for the Ku-Band product). (f) and (g) the same for distance from human land use (as in Figure 5). Country outlines provided by the 'maps' package in R and Amazon Basin outline created from http://worldmap.harvard.edu/data/geonode:amapoly_ivb (see Methods).

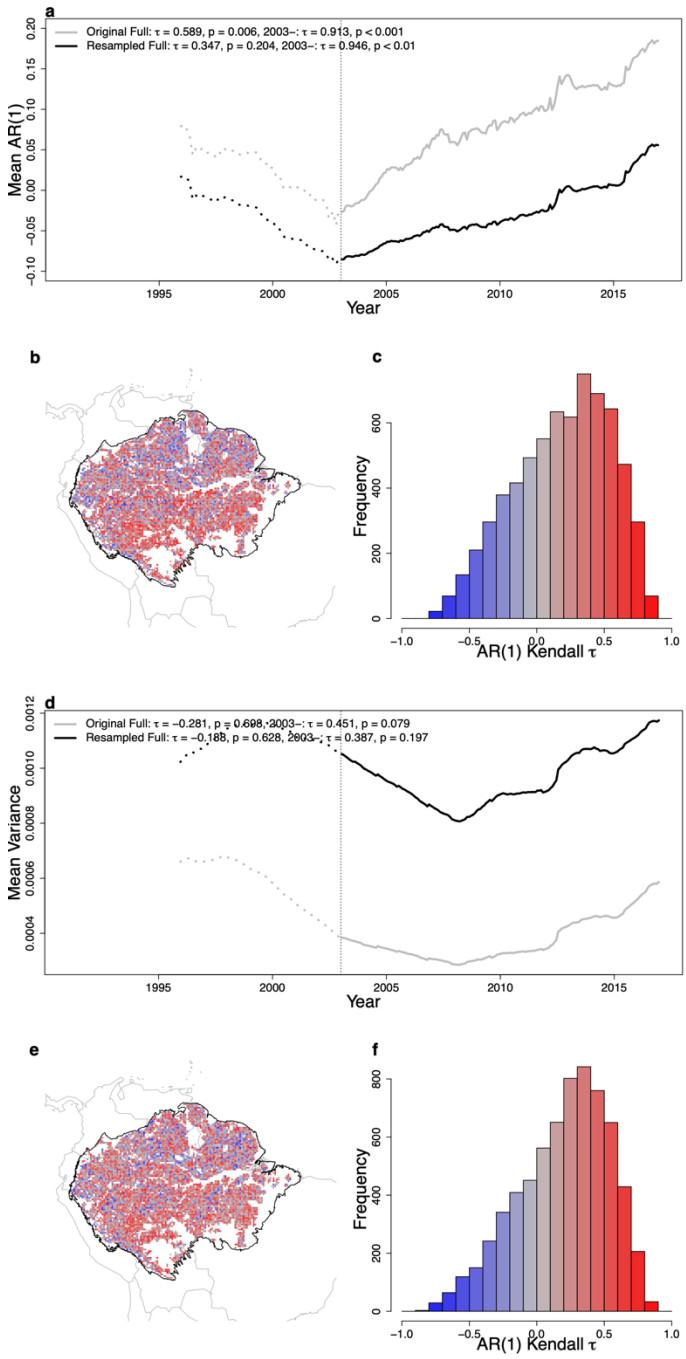

Supplementary Figure S23: Resilience signals calculated from a VOD dataset where a single day each month was sampled. VOD (a) mean AR(1) basin-wide time series for the dataset used in our analysis (grey; as in Figure 2) and when the dataset is resampled such that only a single day each month is used (black). (b) and (c) show the Kendall τ values across the basin and distribution for the resampled dataset from 2003 onwards. (d)-(f) show the same for variance. The relative change in these signals remains similar, showing that the number of satellite passes is not linked to the results we observe. Country outlines provided by the 'maps' package in R and Amazon Basin outline created from http://worldmap.harvard.edu/data/geonode:amapoly_ivb (see Methods).